Design and Analysis of Triple-Band SIW Antenna for K-Band and Ka-Band Applications

Md Mahabub Alam
Faculty of Electrical & Electronics Engineering Technology, Universiti Malaysia Pahang Al-Sultan Abdullah

Ahmad Afif Mohd Faudzi
Faculty of Electrical & Electronics Engineering Technology, Universiti Malaysia Pahang Al-Sultan Abdullah

Syamimi Mardiah Shaharum
Faculty of Electrical & Electronics Engineering Technology, Universiti Malaysia Pahang Al-Sultan Abdullah

Yasmin Abdul Wahab
Faculty of Electrical & Electronics Engineering Technology, Universiti Malaysia Pahang Al-Sultan Abdullah

他

https://doi.org/10.5109/7323346

出版情報：Proceedings of International Exchange and Innovation Conference on Engineering & Sciences (IEICES). 10, pp.760-766, 2024-10-17. International Exchange and Innovation Conference on Engineering & Sciences
バージョン：

Design and Analysis of Triple-Band SIW Antenna for K-Band and Ka-Band Applications

Md Mahabub Alam[1], Ahmad Afif Mohd Faudzi[1],Syamimi Mardiah Shaharum[1], Yasmin Abdul Wahab[1], Muhammad Hazarul Azmeer Ab Malek[3], Mohamad Shaiful Abdul Karim[1] and Nurhafizah Abu Talip Yusof[1,2*]
[1]Faculty of Electrical & Electronics Engineering Technology, Universiti Malaysia Pahang Al-Sultan Abdullah, 26600 Pekan, Pahang, Malaysia
[2]Center for Research in Advanced Fluid & Process (Fluid Center), Universiti Malaysia Pahang Al-Sultan Abdullah, Lebuh Persiaran Tun Khalil Yaakub 26300, Kuantan, Pahang, Malaysia
[3]Tokyo Electric Power Services Co. Ltd (TEPSCO), 1-7-12 Shinonome, Koto City, Tokyo 135-0062, Japan
Corresponding author email: hafizahs@umpsa.edu.my

Abstract: *This paper presents a substrate-integrated waveguide (SIW) antenna designed for K-band and Ka-band applications, addressing propagation and radiation losses at higher frequencies. The proposed patch antenna integrates SIW principles with copper vias and three-ring slots, enhancing the radiation pattern's bandwidth, gain, and stability. Optimized using Computer Simulation Technology (CST) software on a Rogers RT/duroid 5880 substrate (ε_r = 2.2, thickness = 1.575 mm), results in the SIW triple-ring slot patch antenna (SIW-PS3) exhibiting triple-band resonance at 26.066 GHz, 31.552 GHz, and 33.54 GHz, with matching coefficients of -31.96 dB, -47.72 dB, and -21.97 dB, respectively. The SIW-PS3 demonstrates superior performance, including a 9.91% impedance bandwidth (24.826-27.258 GHz), peak gain of 8.072 dB at 26.066 GHz, maximum radiation efficiency of 93%, VSWR between 1 and 5, and directivity ranging from 8.12 to 10.2 dB. These features make it particularly suitable for diverse K-band and Ka-band applications.*

Keywords: Triple band; SIW; patch antenna; 5G antenna; K and Ka-band.

1. INTRODUCTION

Substrate Integrated Waveguide (SIW) technology has revolutionized millimeter-wave wireless communication by addressing previous limitations in handling capacity and bandwidth [1-5]. Conventional patch antennas used for K-band and Ka-band applications often struggle with narrow bandwidth and limited gain, while microstrip arrays, even though effective in increasing data rates, present complex design challenges. With their compact and lightweight structures, SIW antennas [6-11] offer an effective solution by improving signal focus and transmission consistency over long distances. This is crucial for overcoming issues such as rain fade, route loss, and atmospheric attenuation that impact millimeter-wave frequencies in the K-band (18-27 GHz) and Ka-band (27–40 GHz).

Given the critical need to optimize antenna performance to meet these challenges, there is an urgent demand for designs that offer enhanced bandwidth and gain. The evolution of SIW technology reflects this need. Initially, conventional metallic waveguides provided high power handling and low loss but were bulky and non-planar [12]. The second generation, Microwave Integrated Circuits (MIC), introduced strip-like or slot-like planar-printed transmission lines with low-profile structures, sacrificing power-handling capacity and Q-factor for compactness [13-14]. Substrate-integrated waveguides (SIWs) represent a third generation, combining the advantages of both predecessors [15]. SIW structures combine the high power-handling and Q-factors of conventional waveguides with the compactness of MIC structures, bridging planar circuits, and conventional waveguides.
Therefore, this study addresses the pressing need for optimized antenna designs by evaluating various SIW antenna configurations, including the SIW Triple-Ring Slot Patch Antenna (SIW-PS3). By presenting a systematic comparison of several design iterations, this research aims to identify configurations that significantly enhance bandwidth, gain, and efficiency. The findings will contribute to advanced antenna technology and improve high-frequency communication capabilities.

2. Working Principle of SIW

Mechanically, the SIW is a planar structure incorporating a waveguide into a dielectric substrate using two rows of metallic vias to connect the top and bottom conductive layers. These vias are cylindrical, metal-plated holes that penetrate the substrate, forming the SIW's metallic side walls. Fig. 1 shows vias with diameter *d*, spaced at intervals *p*, extending through the substrate from the patch. The design parameters for the SIW guide include the diameter (*d*) of the vias and the spacing (*p*) between them.

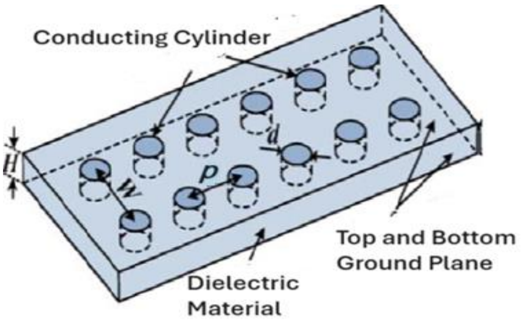

Fig. 1. Structure of SIW [18].

Eq. (1) and (2) highlight key conditions for minimizing electromagnetic energy leakage from via-gaps along narrow walls [16-17].

$$d < \lambda_g/5 \quad (1)$$

$$p \leq 2d \quad (2)$$

Where λ_g is the waveguide's wavelength, d is the diameter of the vias, p is the distance between two vias. The proposed SIW patch antenna design incorporates a circular cavity formed by metallic vias, which serve as sidewalls to confine and guide electromagnetic energy. Optimal via placement and density preserve waveguide integrity, enhance transmission, and reduce losses. This configuration offers a stable platform for K and Ka-band spectrum applications. In a circular waveguide, the dominating modes are the transverse magnetic, TM_{01} and transverse electric, TE_{11} modes, as explained in [19]. Eq. (3) and (4) express the lowest cutoff frequencies for the two dominant modes, TM_{01} and TE_{11}, denoted as $f_{TM_{01}}$ and $f_{TE_{11}}$ respectively. These expressions are derived from solutions to Bessel's differential equation, utilizing the appropriate Bessel functions for each mode:

$$f_{TM_{01}} = \frac{0.383}{a\sqrt{\mu\varepsilon}} \quad (3)$$

$$f_{TE_{11}} = \frac{0.293}{a\sqrt{\mu\varepsilon}} \quad (4)$$

Where a is the radius of the circular waveguide, and μ and ε are the permeability and permittivity of the dielectric material.

The operating principle and design frequency of the cylindrical cavity are established by solving the wave equation within the cavity. This analyzes electromagnetic wave behavior in the cylindrical structure, considering cavity geometry and adaptations for sidewall discontinuities. Eq. (5) and (6) denote that the dominant of TM_{nml} and TE_{nml} mode resonant frequencies, $f_{TM_{nml}}$ and $f_{TE_{nml}}$, in a circular SIW cavity can be calculated as follows

$$f_{TM_{nml}} = \frac{c}{2\pi\sqrt{\mu_r\varepsilon_r}} \sqrt{\left(\frac{P_{nm}}{r}\right)^2 + \left(\frac{l\pi}{h}\right)^2} \quad (5)$$

$$f_{TE_{nml}} = \frac{c}{2\pi\sqrt{\mu_r\varepsilon_r}} \sqrt{\left(\frac{P'_{nm}}{r}\right)^2 + \left(\frac{l\pi}{h}\right)^2} \quad (6)$$

Where, c is the speed of light, P_{nm} and P'_{nm} are the roots of Bessel's function $J_n(x)$ and $J'_n(x)$, a is the radius of the circular cavity, d is the depth, r is the radius of the SIW cavity, and μ_r, ε_r are the permeability and permittivity, respectively.

3. Design Procedure

In this work, the design employs computer simulation technology (CST) software to simulate and analyze four progressive antenna structures, with the basic microstrip patch antenna serving as the base and reference (Fig. 2). The four progressive antenna structures shown in Fig. 3 were built on a basic 20 mm by 15 mm microstrip antenna patch made on a Rogers RT/Duroid 5880 substrate that has a dielectric constant of 2.2 and a thickness of 1.575 mm. The four different designs depicted in Fig. 3 are a single-ring slot patch antenna (PS1), a double-ring slot patch antenna (PS2), a triple-ring slot patch antenna (PS3), and an SIW triple-ring slot patch antenna (SIW-PS3), which is the optimized and proposed design. These antennas evolve through iterative optimization, with each design improving on its predecessor.

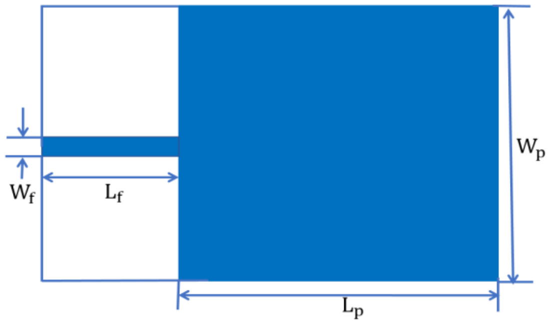

Fig. 2. Basic design of microstrip patch antenna.

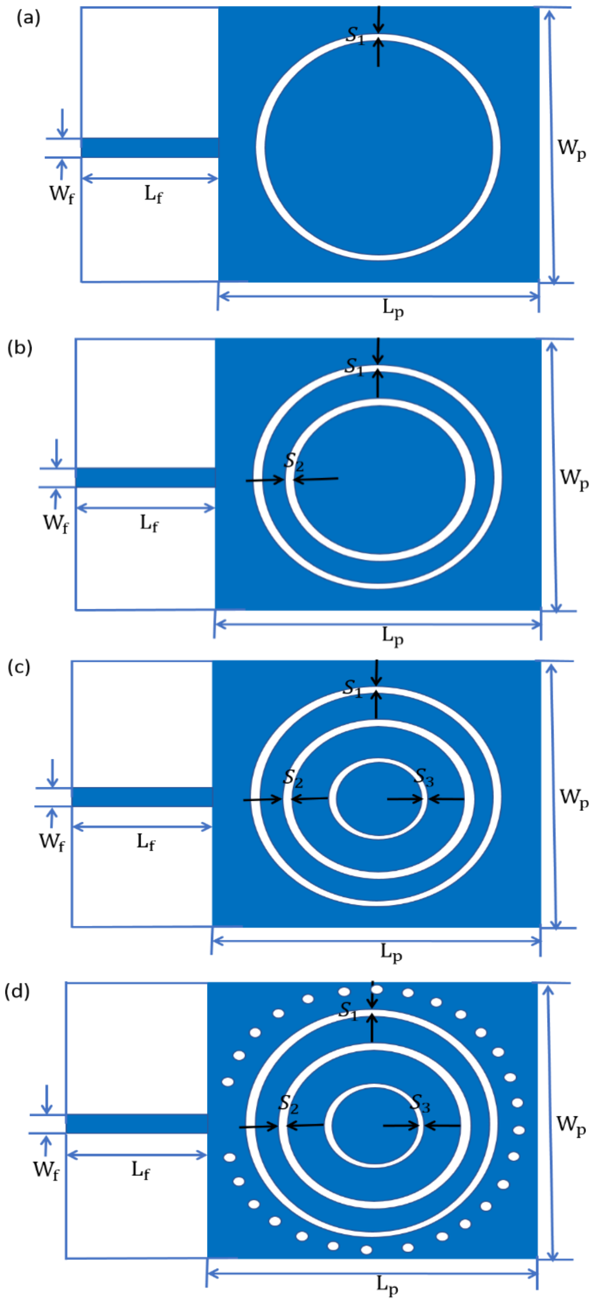

Fig. 3. Design structure of four progressive antennas: (a) single-ring slot patch antenna (PS1), (b) double-ring slot patch antenna (PS2), (c) triple-ring slot patch antenna

(PS3), and (d) SIW triple-ring slot patch antenna (SIW-PS3).

As shown in Fig. 3, the PS1 antenna features a single ring slot etched on a square patch (Fig. 3(a)), while PS2 incorporates double ring slots (Fig. 3(b)). PS3 further enhances the design with triple ring slots (Fig. 3 (c)). The final iteration, SIW-PS3, integrates SIW technology with the triple-ring slot configuration of PS3, aiming to maximize performance improvements (Fig. 3 (d)).

Table 1 presents the optimized and best design parameter dimensions of the SIW-PS3 antenna, which became the proposed design. According to Table 1, the antenna comprises three slots (widths: 0.8 mm, 0.5 mm, 0.5 mm), a 5 mm × 1 mm microstrip feedline and a 20 mm × 15 mm microstrip patch.

Table 1. Optimized dimension of the proposed antenna

Parameter symbol	Parameter description	Dimension (mm)
W_p	Patch width	15
L_p	Patch length	15
d	Via diameter of SIW	0.6
h	Thickness of substrate	1.575
L_f	Length of microstrip feed	5
W_f	Width of Microstrip feed	1
S_1, S_2, S_3	Width of slots 1,2,3	0.8, 0.5, 0.5

4. RESULT AND DISCUSSION

4.1 Analysis of PS1 Antenna Design

Fig. 4 compares the basic microstrip antenna and the PS1 antenna regarding its scattering parameter (S-parameter). The type of S-parameters that have been analyzed is S_{11}, which is known as return loss or reflection coefficient. It measures the difference in power between the incident signal and the reflected signal at the antenna's feed point [21]. Based on the graph, the PS1 antennas outperform the basic microstrip antenna at 26.75 GHz, exhibiting lower return loss and broader bandwidth. Additionally, the PS1 antenna operates efficiently over a more comprehensive frequency range than the basic microstrip patch antenna.

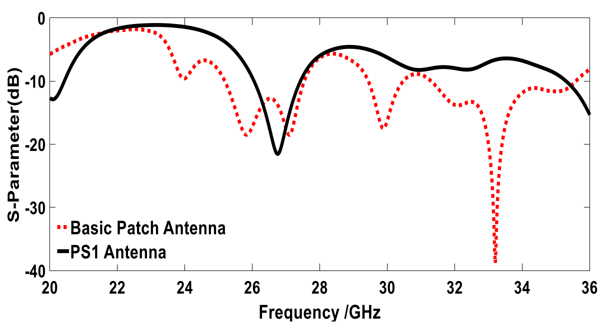

Fig. 4. S-parameter comparison of basic microstrip and PS1 antenna.

Gain is another critical parameter that indicates the antenna's performance. It measures the ability of an antenna to direct or concentrate radio frequency energy in a particular direction. The radiation pattern shows how the antenna radiates power in different directions. It can indicate whether the antenna is omnidirectional (radiating equally in all directions) or directional (radiating more power in specific directions). Figs. 5(a) and (b) presents polar and 3D views of the PS1 antenna's radiation pattern. A polar plot in Fig. 5(a) displays directional gains at specific angles, with black (Phi=0°), blue (Phi=90°), and red (Theta=90°) lines, respectively. The PS1 radiation pattern shows symmetry in the φ = 0° and φ = 90° planes, indicating consistent radiation characteristics in these principal planes. However, $\theta = 90°$ plot shows symmetry except at 90° and 270. Fig. 5(b) presents a 3D visualization of the antenna's gain distribution, employing a color gradient (red for higher gain, blue for lower gain) to depict gain levels in dB across all angles. This 3D visualization reveals the directional characteristics and efficiency of the PS1 antenna. The gain and directivity at 26.75 GHz of the PS1 antenna are 6.97 dB and 8.19 dB, respectively. Maximum efficiency of the PS1 antenna is 84.7%.

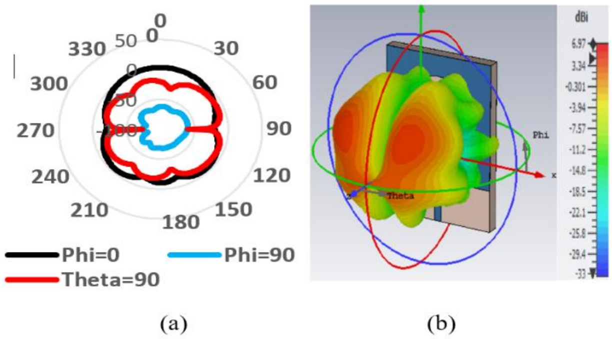

Fig. 5. PS1 antenna radiation pattern at 26.752 GHz (a) Polar. (b) 3D view.

4.2 Analysis of PS2 and PS3 Antenna Design

Fig. 6 compares the S_{11} parameter of PS2 and PS3 antennas, revealing PS3 marginally superior performance at both resonant frequencies. At 26.75 GHz, PS3 achieves a return loss of -22.92 dB compared to -21.56 dB for PS2. At 34.73 GHz, PS3 exhibits a return loss of -14.067 dB versus -12.473 dB for PS2. These lower return loss values for PS3 indicate improved signal reflection reduction and better impedance matching, suggesting slight overall improvement across both frequencies.

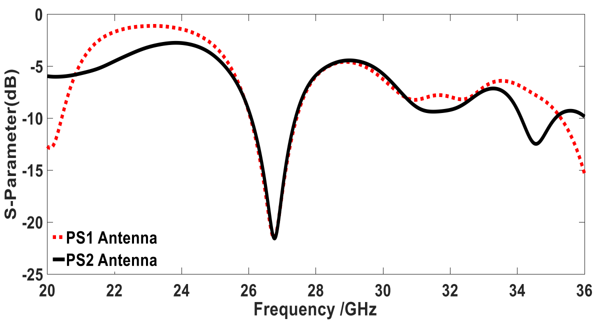

Fig. 6. Analysis result of S_{11} vs. frequency for PS2 and PS3 antenna.

Fig. 7 shows the gain performance of PS2 and PS3 antennas. Both antennas exhibit similar patterns, with multiple peaks between 22-30 GHz, followed by a sharp decline in gain. The PS2 antenna (red dotted line) generally shows a slightly lower gain than the PS3 antenna (black solid line) throughout most of the frequency range. After 30 GHz, both antennas show gain fluctuations, with PS2 peaking sharply approximately at 35 GHz before dropping.

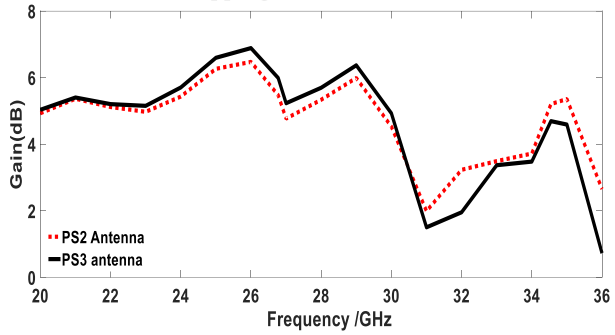

Fig. 7. Comparison of gain for PS2 and PS3 antenna.

4.3 Analysis of Proposed SIW-PS3 Antenna Design

Fig. 8 displays the SIW-PS3 antenna's S_{11} parameter (magnitude in dB) against frequency (GHz) from 20 to 36 GHz, showing critical resonances at 26.066 GHz, 31.552 GHz, and 33.545 GHz. The resonances fall below -10 dB, suggesting effective impedance matching and minimal power loss at these frequencies. To calculate bandwidth, the -10dB point indicates the frequencies over which the antenna performs well.

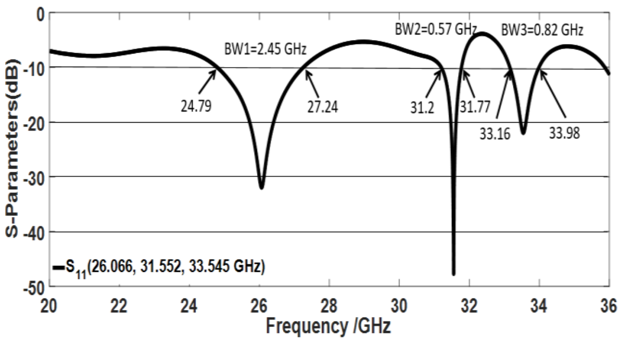

Fig. 8. S-parameter performance of optimized design of SIW-PS3.

The calculated bandwidths for the SIW-PS3 antenna are 2.45 GHz, 0.57 GHz, and 0.82 GHz, with corresponding fractional bandwidths (FBW) of 9.4%, 1.8%, and 2.44%, respectively. Fractional bandwidth (FBW) is expressed in Eq. (7) [22]

$$\text{FBW}=\frac{(f_{max}-f_{min})}{f_c} \times 100\% = \frac{BW}{f_c} \qquad (7)$$

Where f_{max} , f_c and f_{min} is the maximum, center, and minimum frequency of an antenna.

Figure 9 (a), (b), and (c) depict the SIW-PS3 antenna's radiation patterns at 26.066 GHz, 31.552 GHz, and 33.545 GHz, respectively. The polar plots for $\varphi=o^0$ and $\varphi=90^0$ show a more symmetrical, uniform, and rounded pattern, while the pattern is not symmetrical irregular and has variations in different directions for $\theta= 90^0$ at 26.066 GHz, 31.552 GHz, and 33.545 GHz. The 3D radiation patterns use color-coded scales to visualize SIW-PS3 antenna gain in dB comprehensively. The radiation pattern at 26.066 GHz is shown in Fig. 9(a), where higher peak gains of 8.07 dB indicate the antenna's excellent capacity to focus energy in specific directions. Fig. 9(b) and (c), corresponding to 31.552 GHz and 33.545 GHz, respectively, display slightly lower peak gains of 7.66 dB and 6.39 dB. These latter patterns exhibit more irregular shapes, suggesting a less focused energy distribution than the 26.066 GHz case. The SIW-PS3 antenna exhibits excellent efficiency, reaching a peak of 93%.

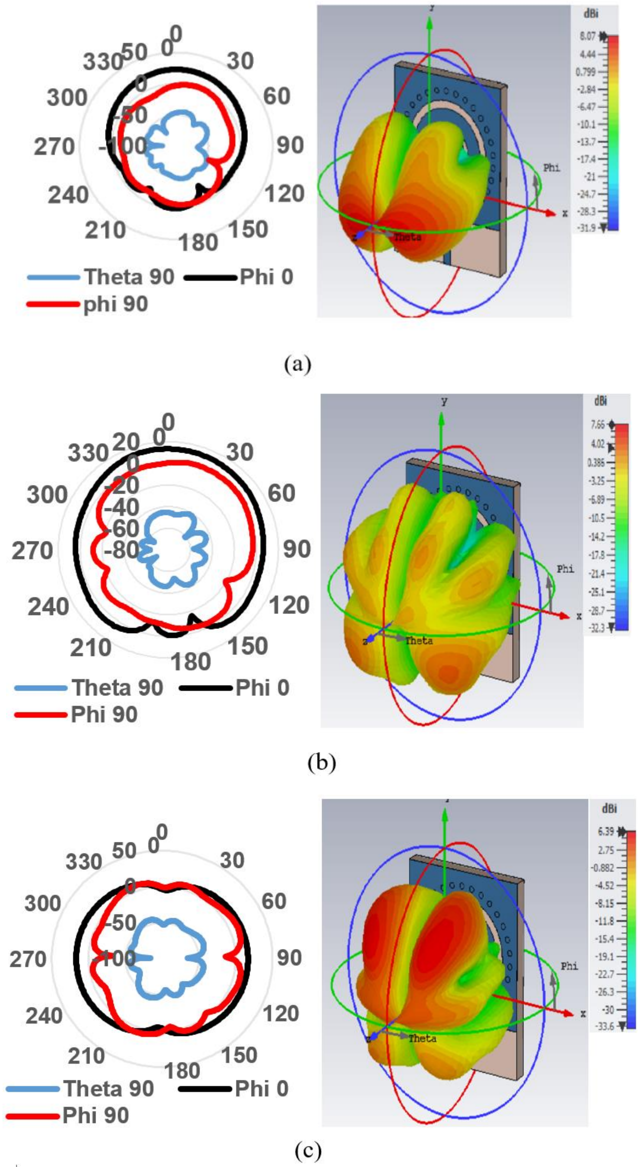

Fig. 9. PS3 antenna radiation Pattern at (a) 26.066 GHz, (b) 31.552 GHz, and (c) 33.545 GHz.

4.4 Surface Current Distribution of SIW-PS3 Antenna

The surface current on an antenna is the electric current distribution on its surface during transmission or reception. This distribution determines the antenna's radiation characteristics. Antenna input impedance, determined by current distribution, must match feed line impedance for efficient power transfer. Fig. 10 (a), (b), and (c) illustrates simulated surface current distributions at 26.066 GHz, 31.552 GHz, and 33.545 GHz, with blue indicating weaker magnetic field intensity and red showing stronger signals. Prominent peaks near slots in inflow and amplitude indicate focused electrical current in these areas. The maximum current flow along slots occurs at 31.552 GHz, and this current distribution ensures minimal loss and maximal radiation efficiency at that frequency. Moreover, the current distribution resonance frequencies exhibit higher intensities around the circular structure's edges, a typical characteristic of patch antennas due to fringing field effects.

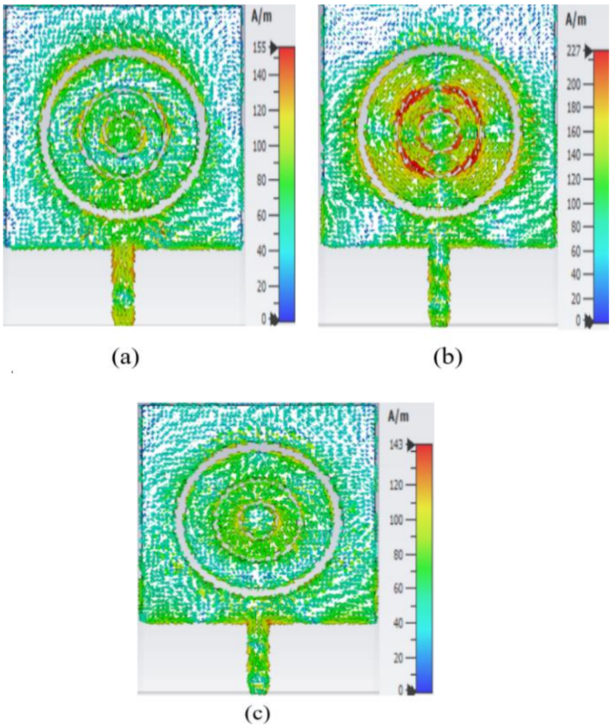

Fig. 10. Surface Current Distribution of SIW-PS3 antenna (a) 26.066 GHz (b) 31.552 GHz (c) 33.545 GHz.

4.5 Comparison of S-Parameter Plots of Different Antenna Designs

Fig. 11 illustrates a comparative analysis of the reflection coefficients for various antenna configurations, including the basic patch, PS1, PS2, PS3, and SIW-PS3 designs across a frequency range from 20 GHz to 36 GHz. The basic patch antenna (red dotted line) exhibits a significant return loss at 33.2 GHz. PS1, featuring a single circular slot, shows limited effectiveness with a resonance at 26.75 GHz and a -21.5 dB return loss. PS2, incorporating two concentric ring slots, demonstrates modest improvement, resonating at 26.775 GHz and 34.576 GHz. PS3 slightly enhances the return loss at both resonant frequencies compared to PS2. However, the SIW-PS3 design, represented by the black line, combines three ring slots with an SIW configuration and exhibits the lowest return loss, indicating superior performance across multiple frequencies compared to other configurations. It exhibits reflection coefficients below -10 dB at multiple points, indicating enhanced impedance matching and lower reflection across a broader frequency spectrum.

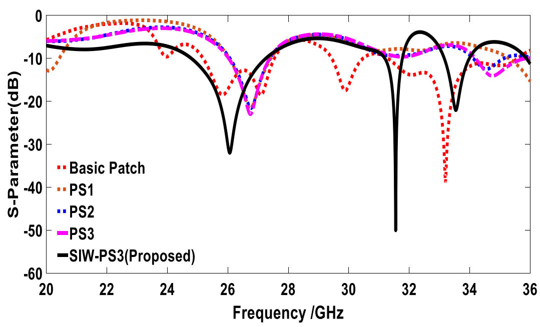

Fig. 11. S-Parameter measurements for different antenna designs.

Table 2 presents a performance comparison of four antenna designs: PS1, PS2, PS3, and SIW-PS3. The comparison covers critical metrics, including operating frequency, S_{11} parameters, bandwidth, and gain. Among these, SIW-PS3 demonstrates superior overall performance. It operates at multiple frequencies (26.067 GHz, 31.552 GHz, and 33.543 GHz), offers the widest bandwidth at 2.458 GHz, and achieves a significant gain of 8.072 dB. These characteristics suggest that SIW-PS3 outperforms the other designs across the measured parameters.

Table 2. Comparison between PS1, PS2, PS3 and SIW-PS3 antenna performance

Design Type	Operating Frequency (GHz)	Return loss(dB)	Bandwidth (GHz)	Gain(dB)
PS1	26.752	-21.536	1.372	6.97
PS2	26.775	-21.564	1.316	7.82
	34.545	-12.473	0.997	7.26
PS3	26.768	-22.925	1.352	8
	34.736	-14.067	1.655	7.66
SIW-PS3	26.067	-31.981	2.458	8.07
	31.552	-50.038	0.57	7.67
	33.543	-22.052	0.817	6.39

4.6 Comparison of VSWR Plots for Best Impedance Matching

The Voltage Standing Wave Ratio (VSWR) measures the ratio of reflected incident waves, which shows how well an antenna transfers power. Lower values suggest better impedance matching and less signal reflection. Fig. 12 shows VSWR measurements for five antenna designs (Basic Patch, PS1, PS2, PS3, and SIW-PS3) across frequencies from 20 GHz to 36 GHz. The SIW-PS3 design (solid black line) shows the most stable and lowest VSWR among the five antennas, indicating the best impedance matching and efficient power transfer compared to others. PS1 (red) and basic patch (blue) designs exhibit the highest VSWR peaks at 22.5 GHz and 23.13 GHz (9.74), respectively, indicating poor performance. PS2 (purple dotted line) and PS3 (magenta dotted line) demonstrate patterns but with lower peak VSWR values compared to Basic Patch and PS1. It is concluded that the SIW-PS3 antenna exhibits superior performance, maintaining consistently low and stable VSWR values across the entire frequency range.

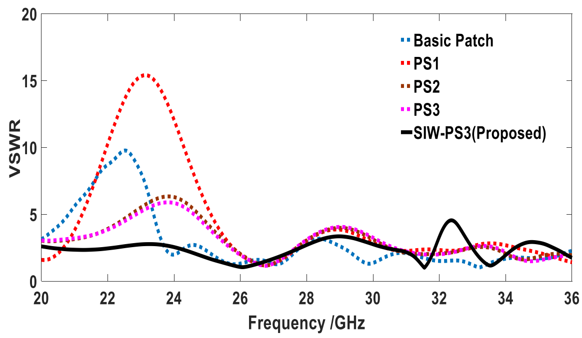

Fig. 12. Comparison of VSWR for Basic Patch, PS1, PS2, PS3, and SIW-PS3 antenna.

4.7 Directivity Analysis for Radiation Pattern Comparison

Fig. 13 displays directivity in decibels (dB) of four antenna designs (PS1, PS2, PS3, and SIW-PS3) across a frequency range of 20 to 36 GHz. The SIW-PS3 design, represented by the black line, shows the highest overall directivity, peaking at 10.2 dB at 26.066 GHz. PS1, PS2, and PS3 designs, shown in blue, red, and pink, respectively, exhibit similar patterns with directivity values generally fluctuating between 4 and 8 dB. All four designs show fluctuations in directivity as the frequency increases, with multiple peaks and troughs throughout the measured range. The SIW-PS3 antenna performs better than the others in most cases, especially between 24 and 28 GHz, where it sends out signals more strongly in one direction.

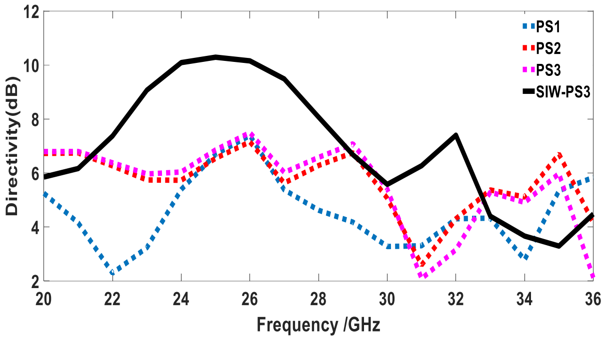

Fig. 13. Comparison of directivity for PS1, PS2, PS3, and SIW-PS3 antenna.

4.8 Comparison with Previous Studies

In this section, we compare our proposed antenna with other recent advancements in SIW antenna design by highlighting the improvements made in our study, as summarized in Table 3. Recent advancements in SIW antenna design have shown promising results for K and Ka-band applications, with several studies focusing on enhancing bandwidth (BW), gain, and radiation efficiency (RE) for these frequency ranges.

For instance, Y. Mahmood Hussein et al. (2020) [23] conducted a comparative study between a microstrip antenna and an SIW microstrip antenna. Their simulation results demonstrated that the SIW antenna, using a Roger RT 5880 substrate with a thickness of 0.508 mm, outperformed the conventional microstrip patch antenna at 28 GHz regarding return loss and radiation pattern. However, despite the superior performance, the gain of 6.4 dB was deemed insufficient for K and Ka-band applications, highlighting the need for further improvements.

Similarly, Almuhsan and Salim (2019) [24] proposed a Ka-band circular patch antenna operating at 30.74 GHz. Their design, while impressive, faced challenges in achieving adequate gain for effective Ka-band satellite communications. This underscores the need for our proposed solution.

Hadi et al. (2020) [25] developed a dual-band circular patch antenna on FR-4 substrate, resonating at 22.45 GHz and 25 GHz. This design achieved bandwidths of 1.20 GHz and 1.50 GHz for the two bands, respectively, with peak gains of 6.14 dB and 4.72 dB. The antenna exhibited good matching characteristics, with return losses of -22.454 dB and -25.106 dB. However, a significant drawback of this design was the relatively low gain, particularly the 4.72 dB peak gain at 25 GHz, which may not be sufficient for applications requiring higher signal strength and long-range communication.

In contrast, our study presents a compact triple-band SIW antenna for K and Ka-band applications. Operating at 26.06, 31.06, and 33.54 GHz, it achieves wide bandwidths and high gains across the three bands. The antenna's exceptional radiation efficiency significantly improves over previous designs, instilling confidence in its potential for K and Ka-band applications.

Table 3. Performance comparison with previous studies

Ref.	Frequency (GHz)	Overall antenna size(mm)	BW (GHz)	Gain (dB)	Max RE (%)
[23]	28	12×12×0.5	1.3	6.4	83.4
[24]	30.74	20×15×0.6	1.176	5.88	76.56
[25]	22.45, 25	20×15×1.5	1.2, 1.5	6.14, 4.72	66.3
This work	26.06, 31.06, 33.54	20×15×1.575	2.45, 0.57, 0.82	8, 7.6, 6.4	93

5. CONCLUSION

This study demonstrates the value of SIW technology in enhancing antenna bandwidth and gain through the analysis of four distinct structures. The optimized SIW-PS3 design achieves triple-band operation with resonances at 26.067 GHz, 31.552 GHz, and 33.545 GHz, covering crucial portions of both K-band and Ka-band spectra. SIW-PS3 significantly outperforms its predecessors (PS1, PS2, and PS3) in terms of reflection coefficient, VSWR, and radiation pattern characteristics. The proposed SIW-PS3 antenna's superior performance, featuring omnidirectional radiation, high gain, and multi-frequency operation in the K/Ka-band, makes it an ideal candidate for satellite and radar systems as well as multi-technology wireless devices, meeting market demands for versatile and high-performance antennas in these frequency ranges. For future approaches, the proposed SIW-PS3 antenna will be fabricated and tested experimentally to verify its performance metrics and compare them with simulated results.

ACKNOWLEDGEMENT

The authors thank the Ministry of Higher Education for providing financial support under Fundamental Research Grant Scheme (FRGS) No. FRGS/1/2022/ST G07/UMP/02/1 (university reference RDU220102) and Universiti Malaysia Pahang Al-Sultan Abdullah for laboratory facilities and additional financial support under Internal Research Grant RDU220382.

6. REFERENCES

[1] A. Elagandula, G. Ram and A. K. Gande, "Design of Dual-Band SIW Cavity Backed Ring Slot Antenna for X/Ka-Band Applications," *2024 IEEE Wireless Antenna and Microwave Symposium (WAMS)*, Visakhapatnam, India, 2024, pp. 1-4

[2] Khair, N. S., Talip Yusof, N. A., Wahab, Y. A., Bari, B. S., Ayob, N. I., and Zolkapli, M. (2023). Substrate-integrated waveguide (SIW) microwave sensor theory and model in characterising dielectric material: A review. *Sensors International*, *4*, 100244.

[3] M. Stanley, Y. Huang, T. Loh, Q. Xu, H. Wang, and H. Zhou, "A high gain steerable millimeter-wave antenna array for 5G smartphone applications," 2017 11th European Conference on Antennas and Propagation (EUCAP), pp. 1311-1314, 2017.

[4] D. Deslandes and K. Wu, "Integrated microstrip and rectangular waveguide in planar form," IEEE Microw. Wireless Compon. Lett., vol. 11, no. 2, pp. 68–70, Feb. 2001.

[5] M. Hussain, N. S., Azman, A. N., Talip Yusof, N. A., Hj Mohtadzar, N. A. A., & A. Karim, M. S. (2022). Design of resonator cavity for liquid material characterization. *TELKOMNIKA (Telecommunication Computing Electronics and Control)*, *20*(2), 447.

[6] P. H. Rao, S. Sujitha, and K. T. Selvan, ''A multiband, multiploidization shared-aperture antenna: Design and evaluation,'' IEEE Antennas Propag. Mag., vol. 59, no. 4, pp. 26–37, Aug. 2017.

[7] Bari, B. S., Khatun, S., Ghazali, K. H., Islam, M., Rashid, M., Rahman, M., & Talip, N. A. (2020). *Performance Comparison of Early Breast Cancer Detection Precision Using AI and Ultra-Wideband (UWB) Bio-Antennas* (pp. 354–365).

[8] Khair, N. S., Yusof, N. A. T., Ariff, M. H. M., Wahab, Y. A., & Bari, B. S. (2022). Recent Advances and Open Challenges in RFID Antenna Applications (pp. 507–517).

[9] F. Xu and K. Wu, ''Guided-wave and leakage characteristics of substrate integrated waveguide,'' IEEE Trans. Microw. Theory Techn., vol. 53, no. 1, pp. 66–73, Jan. 2005.

[10] Shaharum, S. M., Hashim, N. H., Abu Talip @ Yusof, N., Abdul Karim, M. S., & Mohd Faudzi, A. A. (2019). *Automatic Detection of Diabetic Retinopathy Retinal Images Using Artificial Neural Network* (pp. 495–503).

[11] M. Bozzi, A. Georgiadis and K. Wu. "Review of Substrate-integrated waveguide Circuits and Antennas," IET Microw. Antennas Propagation, vol. 5 iss. 8, pp. 909-920, 2011.

[12] Abu Talip @ Yusof, N., Shaharum, S. M., Mohd Faudzi, A. A., Khatun, S., Abdul Karim, M. S., & Hazali, S. F. (2019). *Design of Ultra-Wideband (UWB) Horn Antenna for Non-destructive Fruit Quality Monitoring* (pp. 515–521).

[13] Das, U., & Jahan, N. (2020). A high gain dual band microstrip patch antenna design implementing rectangular slotted electromagnetic band gap structure. Proceedings of International Exchange and Innovation Conference on Engineering & Sciences (IEICES), 6, 60–66.

[14] P. Chaurasia, R. Nigam and M. Bhowmik "SIW Based Slot Antenna In X-Band Using Rogers/RT duroid 5880 As Substrate" International Journal of Materials Science ISSN 0973-4589 Volume 12, Number 1,2017.

[15] A. Dadgarpour, M. S. (2016). Planar High-efficiency Antenna Array using New Printed Ridge Gap Salehi, M., Mehrshahi, E. "A closed-form formula for dispersion characteristics of fundamental SIW mode", IEEE Microwave and Wireless Components Letters, 2011, vol. 21, no. 1, p. 4–6.

[16] M. Salehi, E. M. (2011). A Closed-Form Formula for Dispersion Characteristics of Fundamental SIW Mode. *IEEE microwave and wireless components letters*, 4-6.

[17] Chowdhury, M. H., Hossain, Q. D., Hossain, Md. A., & Cheung, R. C. C. (2019). Single feed circularly polarized crescent-cut and extended corner square microstrip antennas for wireless biotelemetry. International Journal of Electrical and Computer Engineering (IJECE), 9(3), 1902.

[18] Deslandes, D., Wu, K., "Accurate modeling, wave mechanisms, and design considerations of a substrate integrated waveguide", IEEE Transactions on Microwave the Oryand Techniques, 2006, vol. 54, no. 6, p. 2516–2526.

[19] S. Manna (2016). Rectangular Microstrip Patch Antenna for Medical Applications. International Journal of Advanced Research in Electrical, Electronics and Instrumentation Engineering, 698-701.

[20] K. Wu, D. D. (2003.). The Substrate Integrated Circuits - A New Concept for High-Frequency Electronics and Optoelectronics. International Conference on Advanced Technologies, Systems and Services in Telecommunications (TELSIKS) (pp. 3-10). Serbia and Montenegro: IEEE Xplore.

[21] Syefrizal, M. Z. E., Yusof, N. A. T., Karim, M. S. A., Hasan, N., & Zakaria, N. F. (2022). Design of Vivaldi antenna for non-destructive measurement applications. Engineering Technology International Conference (ETIC 2022), 356–363.

[22] Tabassum, S., Shil, A., & Jahan, N. (2020). Wideband Circularly Polarized Metamaterial-based Antenna employing Metasurface Structure. Proceedings of International Exchange and Innovation Conference on Engineering & Sciences (IEICES), 6, 40–45.

[23] Hussein, Y. M., A. Rahim, M. K., Murad, N. A., Jawad, M. M., Hanoosh, H. O., Majid, H. A., & Keriee, H. H. A. (2020). Substrate integrate waveguide and microstrip antennas at 28 GHz. Bulletin of Electrical Engineering and Informatics, 9(6), 2462–2468.

[24] M. A. Abd Almuhsan, A. J. (2019). A Circular Patch Antenna Based Substrate Integrated Waveguide Technology for 5th Generation Systems. IEEE Xplore (pp. 270-273). Baghdad, Iraq: Third Scientific Conference of Electrical Engineering (SCEE).

[25] R. M. Hadi, F. M. (2020). Dual Bands Microstrip Substrate Integrated Waveguide (SIW) Antenna for K-band Applications. Al-Furat journal of innovations in electronics and computer engineering (pp. 2-7). Iraq: Al-Najaf: Al-Furat Al-Awsat Technical University.